Gondwana Research 20 (2011) 243–254

Contents lists available at ScienceDirect

Gondwana Research

journal homepage: www.elsevier.com/locate/gr

Neoproterozoic (~900 Ma) Sariwon sills in North Korea: Geochronology, geochemistry and implications for the evolution of the south-eastern margin of the North China Craton

Peng Peng [a,b,*], Ming-Guo Zhai [a,b], Qiuli Li [a], Fuyuan Wu [a], Quanlin Hou [c], Zhong Li [a], Tiesheng Li [a], Yanbin Zhang [a]

[a] State Key Laboratory of Lithospheric Evolution, Institute of Geology and Geophysics, Chinese Academy of Sciences, Beijing 100029, China
[b] Key Laboratory of Mineral Resources, Chinese Academy of Sciences, Beijing 100029, China
[c] Graduate University of Chinese Academy of Sciences, Beijing 100039, China

ARTICLE INFO

Article history:
Received 22 October 2010
Received in revised form 27 December 2010
Accepted 30 December 2010
Available online 6 January 2011

Keywords:
North China Craton
Neoproterozoic
Korean peninsula
Sill and dyke
Rodinia supercontinent

ABSTRACT

The Sariwon sills are distributed in the Pyongnam basin at the center of the Korean peninsula, eastern part of the North China Craton. These sills are up to 150 m in thickness and up to more than 10 km in length. Baddeleyite grains separated from a ~50 m thick sill give a SIMS ^{206}Pb–^{207}Pb age of 899 ± 7 Ma (MSWD = 0.34, n = 14), which is interpreted to be the crystallization age of this sill. Zircon grains from the same sill gives a lower intercept U–Pb age of ~400 Ma, which is likely a close estimation of the greenschist-facies metamorphism of this sill. The Sariwon sills are dolerites and have tholeiitic compositions. They show enrichment of light rare earth element concentrations (La/Yb_N = 1.4–2.8) and are slightly depleted in high field strength elements (e.g. Nb, Zr, and Ti), in comparison to neighboring elements on the primitive-mantle normalized spidergram. The whole rock εNd_t (t = 900 Ma) values are around −2, whereas *in-situ* εHf_t (t = 900 Ma) values from zircon grains vary from −25 to +8. They are similar to the coeval sills in other parts of the North China Craton, e.g., the Chulan sills (Xu-Huai basin, Shandong peninsula) and the Dalian sills (Lv–Da basin, Liaodong peninsula). These sills possibly originated from a depleted mantle source (e.g., asthenosphere), rather than from the ancient lithospheric mantle of the North China Craton, and have experienced significant assimilation of lithospheric materials. The strata and sills in the Xu-Huai, Lv–Da and Pyongnam basins are comparable; moreover the three basins are geographically correlatable based on Neoproterozoic geographical reconstruction. We therefore propose that there is a Xu-Huai–Lv–Da–Pyongnam rift system along the south-eastern edge of the North China Craton during Neoproterozoic (~900 Ma), with the closure of the rift at ~400 Ma as a result of a continent-margin process. It is possible that this southeastern margin of the NCC did not face the inland in the configuration of the supercontinent Rodinia.

1. Introduction

The North China Craton (NCC) (Fig. 1a), one of the oldest cratons with crustal materials as old as 3.8 Ga (e.g., Liu et al., 1992, 2008; Wu et al., 2008), is also known as the Sino-Korean craton because of its extending into the Korean Peninsula. The eastern border between the NCC and the South China Craton is represented by the Su-Lu orogen in the Shandong Peninsula. This orogen is thought to extend into the central part of the Korean peninsula based on the comparable of Triassic (~230 Ma) eclogite rocks (e.g., Oh et al. 2005; Oh, 2006; Kim et al., 2006, 2009; Zhai et al. 2007), syenite plutons (Peng et al., 2008), metamorphic belts and basin formations (e.g. Ree et al., 1996; Cho, 2001; Oh, 2006; Oh and Kusky 2007; Kwon et al., 2009; Oh et al. 2009; Sajeev et al., 2010), as well as structures (e.g., Yin and Nie, 1993; Hou et al., 2008) and geophysics continuities (e.g., Choi et al., 2006), with those in Shandong Peninsula (Fig. 1a).

Previous geochronology in this border area in the central Korean Peninsula includes several age groups, e.g., ~2500 Ma, 1900−1800 Ma and 230−220 Ma, however, ages of ~900 Ma and ~400 Ma are rarely reported but of great significance (e.g., Cho, 2001; Sagong et al., 2003; Kim et al., 2006; Oh et al., 2009 and reference therein). Oh et al. (2009) interpreted the Neoproterozoic ages to be comparable to those in and around the South China Craton, i.e., either from arc processes or resulted from rifting, as these ages are thought to be absent in the NCC. For the ~400 Ma ages, although Cho (2001) has interpreted a case as of igneous activity, Sagong et al. (2003), Kim et al. (2006) and Oh et al. (2009) interpreted their ~400 Ma ages in the central Korean

* Corresponding author. State Key Laboratory of Lithospheric Evolution, Institute of Geology and Geophysics, Chinese Academy of Sciences, Beijing 100029, China. Tel.: +86 10 82998527.
E-mail address: pengpengwj@mail.iggcas.ac.cn (P. Peng).

1342-937X/$ – see front matter
doi:10.1016/j.gr.2010.12.011

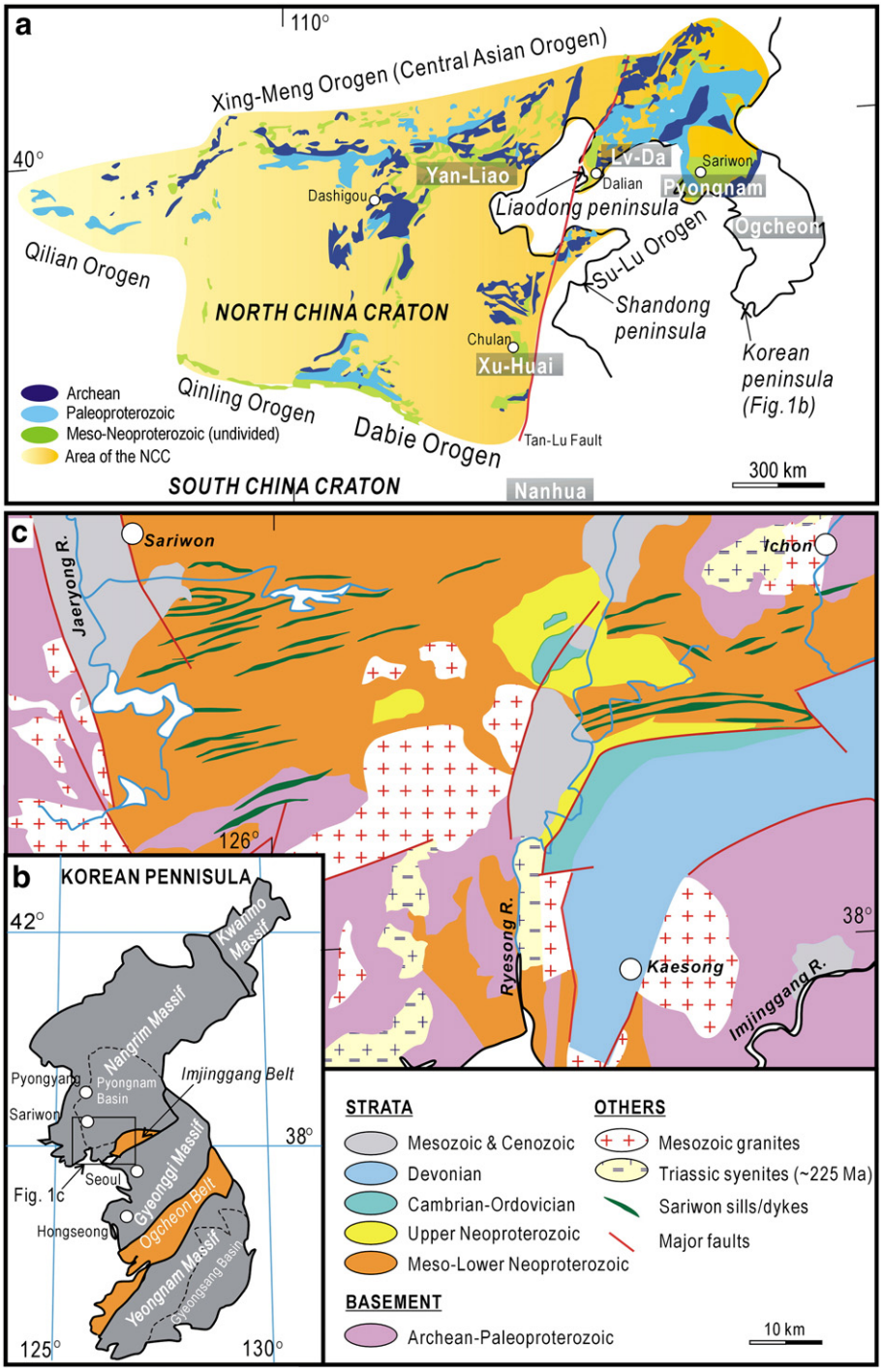

Fig. 1. (a) Archean–Paleoproterozoic basement and Meso-Neoproterozoic cover of the North China craton. (b) Tectonic units of the Korean peninsula (revised after Paek et al., 1996). (c) Simplified geological map showing the Sariwon sills in North Korea.

peninsula to be of granulite—facies metamorphic events recorded in the basement. Kim et al. (2006) have used a Paleozoic collision model to interpret this ~400 Ma event in Korean peninsula as those in the Qinling—Qilian orogen (Fig. 1a; e.g. Sun et al., 2002; Yang et al., 2005).

In this paper, we present geochronologic data on one of the Sariwon sills from the Korean peninsula which gives a Neoproterozoic (~900 Ma) protolith age and a late Silurian-early Devonian (~400 Ma) metamorphic age. The geological significance of the sills, as well as their relationships with coeval associations and basins in other parts of the NCC, are discussed.

2. Geological background

The Korean Peninsula can be subdivided into four (Archean—) Paleoproterozoic massifs (Kwanmo, Nangrim, Gyeonggi and Yeongnam), from north to south (Fig. 1b; e.g., Paek et al., 1996; Chough et al., 2000). Among these, the Kwanmo massif, is an exotic block in the

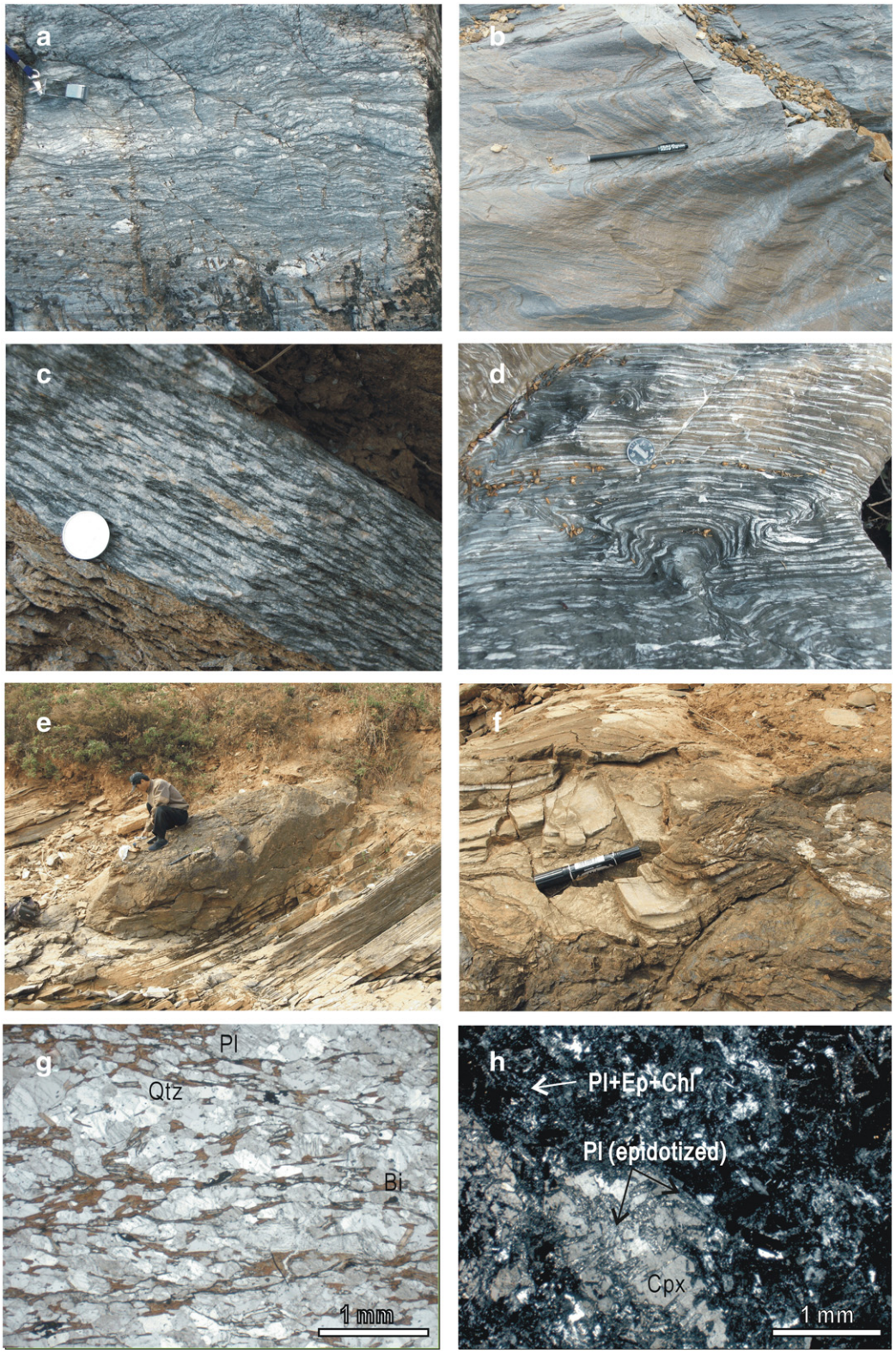

Fig. 2. Selected field photos and photomicrographs of sills and related formations in the Sariwon–Kaesong area: (a) deformed conglomerate; (b) folded beds of the sediments; (c) biotite-schist; (d) deformed limestone; (e) a 3-m thick dolerite sill; (f) a finger of a sill into the sedimentary layers; (g) strongly deformed sandstone (2.5×, plane-polarized light); (h) Sariwon sill (sample 05NK61, 2.5×, cross-polarized light). Chl = chlorite; Ep = epidote; Qtz = quartz; Pl = plagiocalse; Ab = albite; Ap = apatite; Cpx = clinopyroxene. (a), (b), (e), and (f) are strata of the Songwon System, whereas (c) and (d) are of the Imjinggang System. Scale of (a) is a lens about 3 cm in length, scales of (b) and (f) are pens about ~15 cm long, scales of (c) and (d) are a coin about ~2 cm in diameter, scale of (e) is a person about 170 cm tall, and the white scale bars in (g) and (h) are 1 mm in length.

Xing-Meng orogen; the Nangrim massif is a part of the NCC; and the Gyeonggi and Yeongnam massifs could be parts of the South China craton (e.g. Yin and Nie, 1993; Xu and Zhu, 1995; Ree et al., 1996; Chang and Park, 2001; Ishiwatari and Tsujimori, 2003; Oh et al., 2005, 2009; Kim, et al., 2006; Wu et al., 2007). However, Zhai et al. (2007) consider that most parts of the Nangrim, Gyeonggi and Yeongnam

Table 1
U–Pb zircon/baddeleyite SIMS analysis of a Sariwon sill in North Korea.

1A: SHRIMP zircon data

Spot	U [ppm]	Th [ppm]	$^{232}Th/^{238}U$	$^{206}Pb_c$ [%]	$^{206}Pb^*$ [ppm]	$^{207}Pb^*/^{206}Pb^*$	±σ[%]	$^{207}Pb^*/^{235}U$	±σ%	$^{206}Pb^*/^{238}U$	±σ [%]	^{206}Pb–^{238}U age [Ma]	±σ [%]	^{206}Pb–^{207}Pb age [Ma]	±σ	ρ
1	1489	2796	1.94	0.07	159	0.06566	0.9	1.121	2.0	0.1239	1.8	753	±13	795	±18	.90
2	1853	3137	1.75	0.17	155	0.06155	0.9	0.825	2.0	0.0972	1.8	598	±10	659	±20	.89
3	1617	3218	2.06	0.06	179	0.06643	0.8	1.177	2.0	0.1286	1.8	780	±13	820	±17	.91
4	1368	3122	2.36	0.17	121	0.06253	1.1	0.885	2.1	0.1026	1.8	630	±11	692	±23	.86
5	1236	1810	1.51	0.01	139	0.06865	1.1	1.241	2.1	0.1311	1.8	794	±13	888	±23	.85
6	2715	5780	2.20	0.30	160	0.05711	1.2	0.539	2.2	0.0684	1.8	427	± 7	496	±27	.82
7	1451	2921	2.08	0.13	165	0.06559	1.3	1.192	2.2	0.1318	1.8	798	±14	793	±27	.81
8	2306	3269	1.46	0.28	182	0.0615	1.6	0.778	2.8	0.0918	2.3	566	±12	657	±35	.81
9	1847	4056	2.27	0.21	142	0.05973	1.3	0.735	2.2	0.0893	1.8	551	± 9.6	594	±28	.82
10	791	1212	1.58	0.07	92.4	0.06676	1.2	1.251	2.2	0.1359	1.9	821	±14	830	±25	.84
11	964	1215	1.30	0.63	106	0.0660	2.6	1.162	3.2	0.1278	1.9	775	±14	805	±54	.58
12	1479	2478	1.73	0.12	154	0.06472	1.2	1.081	2.2	0.1211	1.8	737	±13	765	±26	.83

1B: CAMECA baddeleyite Pb isotope data

Spot	$^{206}Pb/^{204}Pb$ measured	±σ%	$^{207}Pb/^{206}Pb$ measured	±σ%	$^{207}Pb/^{206}Pb$ corrected	±σ%	^{206}Pb–^{207}Pb age (Ma)	±σ	^{206}Pb (cps)
1	1.98E−05	5.7	0.06919	0.25	0.06898	0.25	898	11	10,089
2	2.19E−05	7.9	0.06860	0.30	0.06836	0.30	879	13	6839
3	2.07E−05	5.1	0.06909	0.27	0.06887	0.27	895	12	9657
4	8.59E−05	2.4	0.06999	0.35	0.06907	0.36	901	15	4691
5	2.84E−05	14.2	0.06908	0.24	0.06878	0.25	892	10	10,656
6	2.84E−05	4.0	0.06941	0.30	0.06911	0.30	902	13	7039
7	4.97E−04	3.7	0.07414	0.38	0.06880	0.50	893	19	5029
8	1.79E−05	14.2	0.06930	0.24	0.06910	0.25	902	10	11,444
9	1.52E−04	4.5	0.07088	0.30	0.06925	0.33	906	14	6583
10	1.75E−04	4.6	0.07098	0.37	0.06910	0.40	902	16	4567
11	3.60E−04	3.2	0.07296	0.26	0.06911	0.33	902	16	8344
12	3.38E−04	3.6	0.07303	0.24	0.06940	0.32	911	13	10,004
13	1.57E−04	6.2	0.07079	0.28	0.06911	0.32	902	13	7833
14	5.33E−04	2.7	0.07478	0.35	0.06906	0.44	901	31	5820

Notes: a. Pb_c and Pb^* indicate the common and radiogenic portions, respectively. b. Common Pb is corrected using measured ^{204}Pb. c. ρ represents error correlation coefficient.

massifs belong to the NCC, and that the suture zone of the NCC and South China craton is present in the westernmost domain of the central part of the Korean peninsula.

Several other units, e.g., the Imjinggang belt, the Ogcheon belt (including the Taebaeksan basin), the Gyeongsang basin and the Pyongnam basin, are developed on the above massifs (Fig. 1b; e.g., Paek et al., 1996; Chough et al., 2000). The Imjinggang belt is tectonically overlain on the south side of the Pyongnam basin; and is composed of strongly deformed Cambrian—Devonian siliciclastic and carbonate metasedimentary sequences (Fig. 1c; e.g., Cho et al., 1995; Paek et al., 1996; Ree et al., 1996). The Ogcheon belt is a fold-and-thrust belt dominated by Neoproterozoic–Paleozoic metasediments and metavolcanics (~756 Ma) and is located between the Gyeonggi and Yeongnam massifs (Fig. 1c; e.g. Lee et al., 1998; Fitches and Zhu, 2006). The peak metamorphic age of the Ogcheon belt is suggested to be at Permian–Early Triassic (e.g., Chough et al., 2000; Cheong et al., 2003). The Gyeongsang basin is the Cretaceous dominated succession evolved on the basement of the Yeongnam massif (e.g. Chun and Chough, 1992).

The Pyongnam basin is situated on the Nangrim massif, and composed of a 7000–8000 m thick greenschist-facies metasedimentary sequence (e.g., schists, quartzites, marbles, and meta-calc-silicates). Two systems have been distinguished, i.e., the Songwon System (Jikhyon, Sadangu, Mukchon, and Myoraksan Groups) and the Kuhyon System (Pirangdong and Rungri Groups) in order from bottom to top (Paek et al., 1996). The Jikhyon Group composes of conglomerate, quartzite, marble, and phyllite, and is about 3000 m in thickness. The

Table 2
Lu–Hf zircon analysis of a Sariwon sill in North Korea.

Spot	Age [Ma]*	$^{176}Lu/^{177}Hf$	$^{176}Hf/^{177}Hf$	2σ	$^{176}Hf/^{177}Hf_i$	εHf_{t1}**	εHf_{t2}***	2σ	T_{DM}	$f_{Lu/Hf}$
1	795	0.001169	0.281526	0.000055	0.281507	−24.9	−27.2	1.9	2430	−0.96
2	659	0.007903	0.282325	0.000066	0.282192	−0.7	−4.8	2.3	1606	−0.76
4	692	0.008114	0.282509	0.000095	0.282370	5.7	2.2	3.4	1300	−0.76
5	888	0.006581	0.282492	0.000068	0.282382	6.0	5.8	2.4	1266	−0.80
6	496	0.010334	0.281886	0.000156	0.281709	−17.7	−23.8	5.5	2548	−0.69
7	793	0.007346	0.282557	0.000095	0.282430	7.9	6.0	3.4	1187	−0.78
8	657	0.011725	0.282265	0.000071	0.282069	−5.1	−8.6	2.5	1948	−0.65
9	594	0.015067	0.282410	0.000088	0.282155	−2.0	−5.7	3.1	1901	−0.55
10	830	0.007410	0.282237	0.000074	0.282125	−3.5	−4.7	2.6	1728	−0.78
12	765	0.001076	0.281581	0.000053	0.281561	−22.9	−25.8	1.9	2348	−0.97

Notes: $\varepsilon Hf_t = 10{,}000 \times \{[(^{176}Hf/^{177}Hf)_{sample} - (^{176}Lu/^{177}Hf)_{sample} \times (e^{\lambda t} - 1)]/[(^{176}Hf/^{177}Hf)_{CHUR} - (^{176}Lu/^{177}Hf)_{CHUR} \times (e^{\lambda t} - 1)] - 1\}$.
$T_{DM} = 1/\lambda \times \ln\{1 + [(^{176}Hf/^{177}Hf)_{sample} - (^{176}Hf/^{177}Hf)_{DM}]/[(^{176}Lu/^{177}Hf)_{sample} - (^{176}Lu/^{177}Hf)_{DM}]\}$.
$f_{Lu/Hf} = (^{176}Lu/^{177}Hf)_{Sample}/(^{176}Lu/^{177}Hf)_{CHUR} - 1$.
The $^{176}Hf/^{177}Hf$ and $^{176}Lu/^{177}Hf$ ratios of chondrite (CHUR) and depleted mantle (DM) at the present day are 0.282772 and 0.0332, and 0.28325 and 0.0384, respectively (Blichert-Toft and Albarède, 1997; Griffin et al., 2000). $\lambda = 1.867 \times 10^{-11}\ a^{-1}$ (Söderlund et al., 2004).
* ^{206}Pb–^{207}Pb ages from Table 1A.
** εHf_{t1} values are calculated using t = 900 Ma.
*** εHf_{t2} values are calculated using ages obtained by SHRIMP analyses (data of the 2nd column).

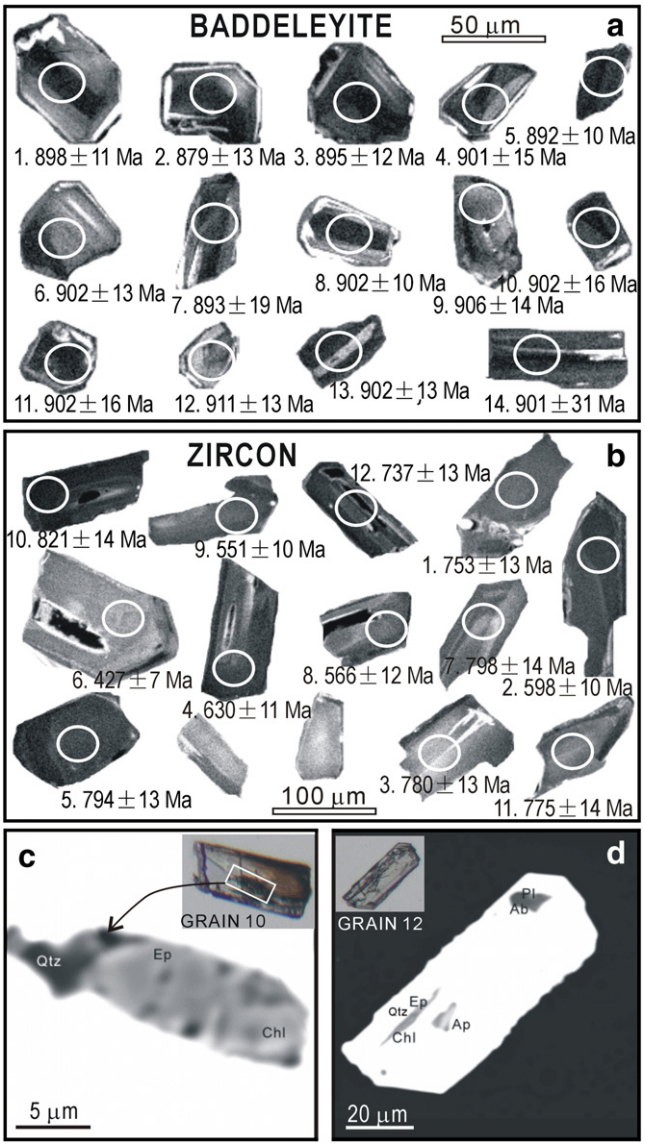

Fig. 3. Selected cathodoluminescence (CL) and backscattered electron (BSE) images of baddeleyite and zircon grains from sample 05NK61. a) Baddeleyite grains (CL). b) Zircon grains (CL). c) and d) Mineral inclusions in zircon grains (grains 10 and 12, see Fig. 3b; BSE). Chl = chlorite; Ep = epidote; Qtz = quartz; Pl = plagiocalse; Ab = albite; Ap = apatite.

Sadangu Group contains massive dolomite, with some limestone layers. The strata is about 1600–2200 m thick. The Mukchon Group is composed of phyllite, quartzite, argillaceous limestone, and is 1200–1500 m thick. The Myoraksan Group is made of dolomite, limestone and phyllite, about 1100–1400 m. The Pirangdong and Rungri Groups are composed of conglomerate, phyllite, shale, dolomite and siltstone, with a total thickness of about 1600–2000 m. Paek et al. (1996) suggested that this sequence is comparable to those in basins from the interior of the NCC, especially to that in the Yan-Liao Basin, which is subdivided into the Changcheng, Jixian (or Gaoyuzhuang and Jixian) and Qingbaikou Systems from bottom to top, and is composed of clastic sediments up to 10,000 m thick with minor volcanics (Lu et al., 2008; Gao et al., 2008; Qiao et al., 2007). Two groups of precisely dated zircon U–Pb ages constrain the timing of the Yan–Liao basin sequence, the ages of volcanics in the Donghongyu Fm. (Changcheng System) (e.g., 1625±6 Ma; Lu and Li, 1991) and the tuff beds in the Xiamaling Fm. (Qingbaikou System) (1368±12 and 1370±11 Ma; Gao et al., 2007, 2008). However, new detrital age data (Li et al., personal communication) suggest that the Songwon and Kuhyon Systems in the Pyongnam basin show very late Mesoproterozoic detrital zircon ages, and thus have a depositional age younger than that of the Yan-Liao sequence.

3. Occurrence and petrography

The Sariwon sills, as well as a few dykes, also known as the Yonsan Complex (e.g. Paek et al., 1996), are distributed in the southern part of the Nangrim massif, mainly in the Pyongnam basin (Fig. 1c). Many of these appear as sills intruded the Songwon System and the Archean–Paleoproterozoic basement (Fig. 1c). They are overlain by the upper Neoproterozoic Kuhyon System and the Phanerozoic strata (Ryu et al., 1990; Paek et al., 1996). No age data are available for these sills. They vary in thickness from a couple of meters to ~150 m, and in length from a couple of kilometers to over 10 km (Paek et al., 1996). Their

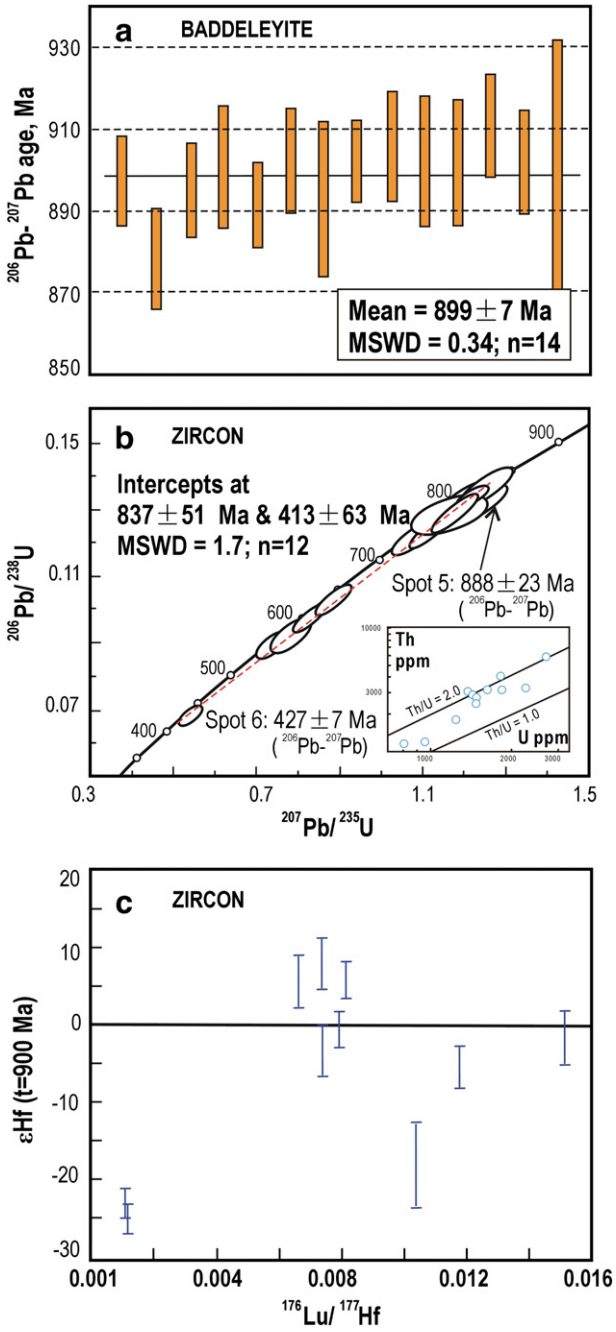

Fig. 4. ^{206}Pb–^{207}Pb age plot (a: baddeleyite), concordia U–Pb age diagram (b: zircon; inset : Th versus U plot), and Lu/Hf versus εHf_t ($t = 900$ Ma) plot (c: zircon) for sample 05NK61 from a Sariwon sill.

Table 3
Major and trace element data and Sr–Nd isotopes of Sariwon sills in North Korea.

3A: major (wt%) and trace element (ppm) data

Sample	SiO_2	TiO_2	Al_2O_3	FeOt	MnO	MgO	CaO	Na_2O	K_2O	P_2O_5	LOI	TOTAL	Mg#	Rb	Sr	Ba	Th	U	Pb	Zr	Hf	Nb	Ta	Sc	V
05NK60	46.45	2.12	14.22	12.9	0.19	6.33	10.58	2.32	1.01	0.32	2.5	98.9	56	24.1	408	549	2.00	0.50	3.66	123	3.38	10.27	0.55	29.2	249
05NK61	47.26	2.37	14.25	13.6	0.21	6.20	10.39	2.34	1.01	0.35	1.98	100.0	54	23.0	431	553	2.51	0.58	8.30	141	3.82	10.00	0.51	31.3	280

3B: Sr–Nd isotope data

SampleNo.	Rb [ppm]	Sr [ppm]	$^{87}Rb/^{86}Sr$	$^{87}Sr/^{86}Sr$	2σ	$^{87}Sr/^{86}Sr_t$	2σ	Sm [ppm]	Nd [ppm]	$^{147}Sm/^{144}Nd$	$^{143}Nd/^{144}Nd$	2σ	εNdt	2σ	fSm/Nd	TDM
05NK60	18.66	417.15	0.1294	0.708310	0.000011	0.7066	0.0005	5.21	23.02	0.1369	0.512204	0.000018	−1.6	0.8	−0.30	1.9
05NK61	18.39	432.83	0.1229	0.709650	0.000011	0.7080	0.0005	5.72	25.59	0.1351	0.512176	0.000009	−1.9	0.7	−0.31	1.9

Notes: a. FeOt: total iron. b. LOI = Loss On Ignition. c. Mg#: Mg number (= 100 $Mg/(Fe^{2+}+Mg)$). d. La/Yb_N and Gd/Yb_N values are La/Yb and Gd/Yb ratios normalized to chondrite values after Sun and McDonough (1989). e. εNd_0 is the present day value, and εNd_t and $^{87}Sr/^{86}Srt$ values are calculated back to 900 Ma. f. T_{DM} ages are calculated after DePaolo (1981).

orientations follow the local foliations, which are dominantly N–NE. A few dykes, having similar petrographic natures with the sills, are seen distributed in the Nangrim massif, and are believed to be belonging to a same swarm (e.g., Paek et al., 1996).

The Sariwon sills are composed of dolerites, with a mineral assemblage of mainly clinopyroxene (partially altered to hornblende) and plagioclase. The rocks experienced greenschist-facies metamorphism and were deformed with the country rocks (Paek et al., 1996). The typical metamorphic assemblage is chlorite, epidote and albite (Appendix A).

Deformation fabrics present in the metasediments of the Pyongnam basin include σ-structure, augen structure, and asymmetrical folds (Fig. 2). All these structures indicate a top to north thrust, according to present coordinates. Fig. 2d shows deformation in the shell-fossil-bearing limestone of the Imjinggang System. Fig. 2e shows a sill intruding into the sediment. Fig. 2f shows a sill finger into the sandstone of the Jikhyon Group. Thin-section photographs of representative sedimentary rocks and a Sariwon sill show deformed fabrics (Fig. 2g) and altered mineral assemblages (Fig. 2h), respectively.

4. Sampling and analytical methods

Sample 05NK61 is from the centre of a 50 m thick sill, located about 30 km east of the Sariwon county (GPS locality: 38°25′ N, 126°02′ E). Both baddeleyite and zircon grains were separated using conventional separation techniques. Baddeleyite Pb–Pb dating was performed on a CAMECA IMS 1280 machine at the Institute of Geology and Geophysics, Chinese Academy of Sciences (IGGCAS), and zircon U–Pb age dating was done on a SHRIMP II machine housed at the Beijing SHRIMP Center (Table 1).

About 23 zircon and 18 baddeleyite grains/broken fragments were mounted in an epoxy resin mount, together with standard Temora 1 zircons with a conventionally measured ^{206}Pb–^{238}U age of 417 Ma (Black et al., 2003). The mount was polished to expose the centers of the grains, and then gold coated. Optical microscope images and cathodoluminescence electron images were acquired in order to examine the shapes and internal textures of the mineral grains. The diameters of the analytical ion beams used in this study are ~15 μm for CAMECA and ~30 μm for SHRIMP. All data were processed using the Squid 1.02 and Isoplot 3.0 programs (Ludwig, 2002, 2003). Analytical procedures for CAMECA and SHRIMP determinations were follow those described in Li et al. (2009a) and Williams (1998), respectively.

In situ Hf isotope analyses were performed on zircon grains of sample 05NK61 on a Neptune MC-ICPMS in the IGGCAS (Table 2). A 63 nm spot size was applied during ablation with a laser repetition rate of 10 Hz. Data processing and correction were after Wu et al. (2006). The baddeleyite grains from this sample are too thin and have failed for analysis.

Whole-rock chemistry analyses were performed at the IGGCAS. Major element determinations were performed by X-ray fluorescence (Shimadzu XRF-1700/1500). The precision was better than 0.2 wt.% in the analysis range. The loss on ignition was measured as the weight loss of the samples after 1 h baking under a constant temperature at 1000 °C. Trace element analyses were determined using an ELEMENT ICP-MS after HNO_3 + HF digestion of about 40 mg of sample powder in a Teflon vessel, with accuracy and reproducibility monitored using the Chinese national standard basalt sample GSR3. The relative standard deviation was better than 5% above the detection limits. Whole-rock Sr–Nd isotope determinations were performed using a Finnigan MAT 262 spectrometer. Standard materials NBS987 and Ames were used as references to quantify analytical bias of the Sr and Nd isotopes, respectively. Procedural blanks for Sr and Nd isotope analyses were better than 100 and 50 pg, respectively. The external precisions (2σ) of $^{87}Rb/^{86}Sr$ and $^{147}Sm/^{144}Nd$ ratios were both better than 0.5%.

The samples analyzed in this study experienced greenschist-facies metamorphism, which could possibly modify whole-rock chemistry selectively, manifested most obviously by high loss-on-ignition (LOI) values, as well as some scattering of major elements, and addition or subtraction of the large ion lithophile elements (LILE) (e.g., Rb, Sr, and Ba) (Chesworth et al., 1981; Middelburg et al., 1988; Pandarinath et al., 2008). However, high field-strength elements (HFSE) and rare earth elements (REE) are relatively immobile during metamorphism, and in general tend to preserve the history of igneous processes (e.g., Middelburg et al., 1988; Pandarinath et al., 2008).

5. Results

5.1. U–Pb and Lu–Hf data

Baddeleyite grains from sample 05NK61 are about 50 μm in length, and are tabular and brownish (Fig. 3a). It is well known that baddeleyite is a potential mineral for Pb–Pb dating but not ideal for Pb–U dating by Secondary Ion Mass Spectrometer (SIMS) owing to the 'crystal orientation effect' that bias the Pb/U isotopic ratio during analysis (Wingate and Compston, 2000). Li et al. (2010) introduced an oxygen flooding technique on a CAMECA IMS 1280 machine, in combination with multi-collector mode and a nuclear magnetic resonance magnet controller, to improve the precision of Pb isotope determinations in baddeleyite. The data in Table 1A are based on these revised techniques, and they yield a weighted average ^{206}Pb–^{207}Pb age of 899 ± 7[2σ] Ma (MSWD = 0.34, n = 14) (Fig. 4a). As the baddeleyite crystallizes generally in the late-stage of mafic magmas, and can

Cr	Co	Ni	Cu	Be	Ga	Cs	Bi	Li	La	Ce	Pr	Nd	Sm	Eu	Gd	Tb	Dy	Ho	Er	Tm	Yb	Lu	Y	REE	La/Yb_N
64.8	43.8	69.5	73.5	0.76	19.5	1.16	0.03	23.7	21.3	45.8	5.94	24.9	5.63	2.08	5.62	0.87	4.74	0.96	2.52	0.37	2.25	0.33	24.8	148	2.34
63.5	44.1	61.6	75.2	0.90	20.0	1.08	0.03	20.9	23.8	52.5	6.86	27.2	6.28	2.17	6.00	0.94	5.45	1.07	2.87	0.40	2.53	0.36	26.9	165	2.33

survive high grades of metamorphism (Heaman and LeCheminant, 1993), this baddeleyite age could be crystallization age of the rock.

Zircon grains from sample 05NK61 are quite thin and small (30–150 μm in lengths), elongated, and are euhedral to sub-euhedral (Fig. 3b). They lack rhythmic zoning and mostly are homogeneous. Some of them have mineral inclusions, with a typical assemblage of chlorite, epidote, feldspar and quartz (Fig. 3cd; Appendix A). They contain high Th (1212–4056 ppm) and U contents (791–2715 ppm), and high Th/U ratios (1.3–2.3). 12 grains were successfully analyzed on a SHRIMP II machine. The U–Pb results fall along a discordant line on the concordia diagram (Fig. 4b). This line yields an upper intercept at 837 ± 51[2σ] Ma, and a lower intercept at 413 ± 63[2σ] Ma (MSWD = 1.7). Spot 5 gives the largest ^{206}Pb–^{207}Pb age of 888 ± 23 Ma [1σ]. The upper intercept age is similar to the age given by baddeleyite grains, and thus could record similar event, whereas the lower intercept age (~400 Ma) could be attributed to Pb loss during the metamorphism of the sill as all the spots distributed along a disconcordant line pointing to ~400 Ma. Initial Hf isotopes for the zircon grains are varied, and as the grains are quite thin, *in-situ* Hf isotope data yield large errors (Table 2, Fig. 4c).

5.2. Whole-rock chemistry

The samples analyzed in this study have TiO_2 contents of 2.12–2.37 wt.%, FeOt (total iron) contents of 12.9–13.6 wt.%, MgO contents of 6.20–6.33 wt.%, total alkali ($Na_2O + K_2O$) contents of 3.33–3.35 wt.% (Table 3). They are tholeiitic (Fig. 5ab), and have enriched rare earth element (REE) concentrations compared to those in chondrite (over 10 times), especially the light REEs (La/Yb_N = ~2.33, normalized to chondrite compositions given by Sun and McDonough, 1989) (Table 3, Fig. 5c). On the primitive mantle normalized trace element spidergram (Fig. 5b), they exhibit a slight depletion in high field strength elements (HFSEs) (e.g. Nb, Zr and Ti), comparing with the neighboring elements (Fig. 5d). Their initial $^{87}Sr/^{86}Sr$ values are about 0.7066–0.7080, and their εNd_t values (t = 900 Ma) are of −1.9 and −1.4 (Table 3, Fig. 6).

6. Discussion

6.1. Comparison of coeval sills in other parts of the NCC

There are several dyke and/or sill swarms which have ages close to those of the Sariwon sills, e.g. the Laiwu dykes (Hou et al., 2005), the Chulan sills (and dykes) (Liu et al., 2006), and the Dalian sills (and dykes) (Yang et al., 2004, 2007 and personal communication) in the eastern NCC, and the Dashigou dykes in the central NCC (~920 Ma, baddeleyite age; Peng, 2010) (Fig. 7).

The Chulan sills are about 10 to 150 m thick and have an NE trend, consistent with the trends of the sediments, and they are tholeiitic in composition. They are mainly dolerites with a mineral assemblage of clinopyroxene and plagioclase (Pan et al., 2000a, b; Liu et al., 2006). K–Ar ages ranging from 586 to 723 Ma are reported (Pan et al., 2000a and reference therein). Liu et al. (2006) obtained average zircon ^{206}Pb–^{207}Pb ages of 1038 ± 26 [2σ] Ma (sample T0398-2) and 976 ± 24 [2σ] Ma (sample T0398-1) using the SIMS method for these sills. However, we notice that the spots of the two samples have very dispersed ^{206}Pb–^{207}Pb ages (for example, sample T0398-2 has ^{206}Pb–^{207}Pb ages that range from 566 Ma to 1433 Ma, and sample T0398-1 has ^{206}Pb–^{207}Pb ages ranging from 788 to 1184 Ma). However, the ^{206}Pb–^{238}U ages are more tightly grouped. Except for two analyses, which have concordia coefficients <0.9, the other 30 analyses of from sample T0398-1 yield a weighted average ^{206}Pb–^{238}U at 910 ± 17[2σ] Ma (n = 30, MSWD = 5.0). Apart from 6 other dispersed spots, the remaining 24 analyses of sample T0398-1 give a weighted average ^{206}Pb–^{238}U age of 918 ± 8[2σ] Ma (n = 24, MSWD = 0.65). As the given $^{206}Pb/^{238}U$ values have smaller errors than those of the corresponding $^{207}Pb/^{206}Pb$ values (see Liu et al., 2006), the ^{206}Pb–^{238}U ages provide a better estimate of the age. In addition, the measured common ^{206}Pb is low (20 analyses are <0.1%, but only 5 analyses are >0.2; see Liu et al., 2006), and the common lead correction will have little effect on the ^{206}Pb–^{238}U ages. Thus the 918 ± 8 Ma age averaged from the ^{206}Pb–^{238}U ages could be used as the estimation of the crystallization age of the sill. This age is similar to that of the Sariwon swarm shown in this paper.

Yang et al. (2004, 2007) have mentioned a swarm in Dalian, Liaoning Peninsula (called as Dalian swarm here; Figs. 1a and 7). This swarm is distributed around the Lv–Da (Lvshun–Dalian) basin area (Fig. 7), and is comprised mostly of sills up to 300 m in thickness, with possibly a few dykes. They are deformed together with the sediments, and metamorphosed to greenschist-facies. The rocks are dolerites and dominated by clinopyroxene and plagioclase (BGMRL, 1989). They are tholeiitic, and chemically similar to the Chulan and Sariwon sills (Fig. 5). Yang et al. (2004) reported ~900 Ma SHRIMP zircon ages from this swarm (weighted ^{206}Pb–^{207}Pb average age at 904 ± 15 [2σ] Ma and weighted ^{206}Pb–^{238}U age at 876 ± 29 [2σ] Ma), although one grain gave a Triassic age (211 ± 2[1σ] Ma). Recently, baddeleyite dating confirmed a ~900 Ma intrusion age for these sills (e.g., weighted CAMECA ^{206}Pb–^{207}Pb average age at 907 ± 4[2σ] Ma and 872 ± 3[2σ] Ma; Yang J.-H., et al., personal communication).

The coeval Sariwon, Chulan and Dalian sills have similar mineral assemblage and chemical compositions, e.g., major element concentrations, REE and trace element concentrations and patterns (Fig. 5), and Sr–Nd isotopes (Fig. 6). These swarms are distributed proximal to the Tan-Lu fault, a major trans-current intra-continental fault zone with over 700 km sinistral displacement, along which most of the offset took place in the Cretaceous (Xu et al. 1987; Xu, 1993). If we reverse this

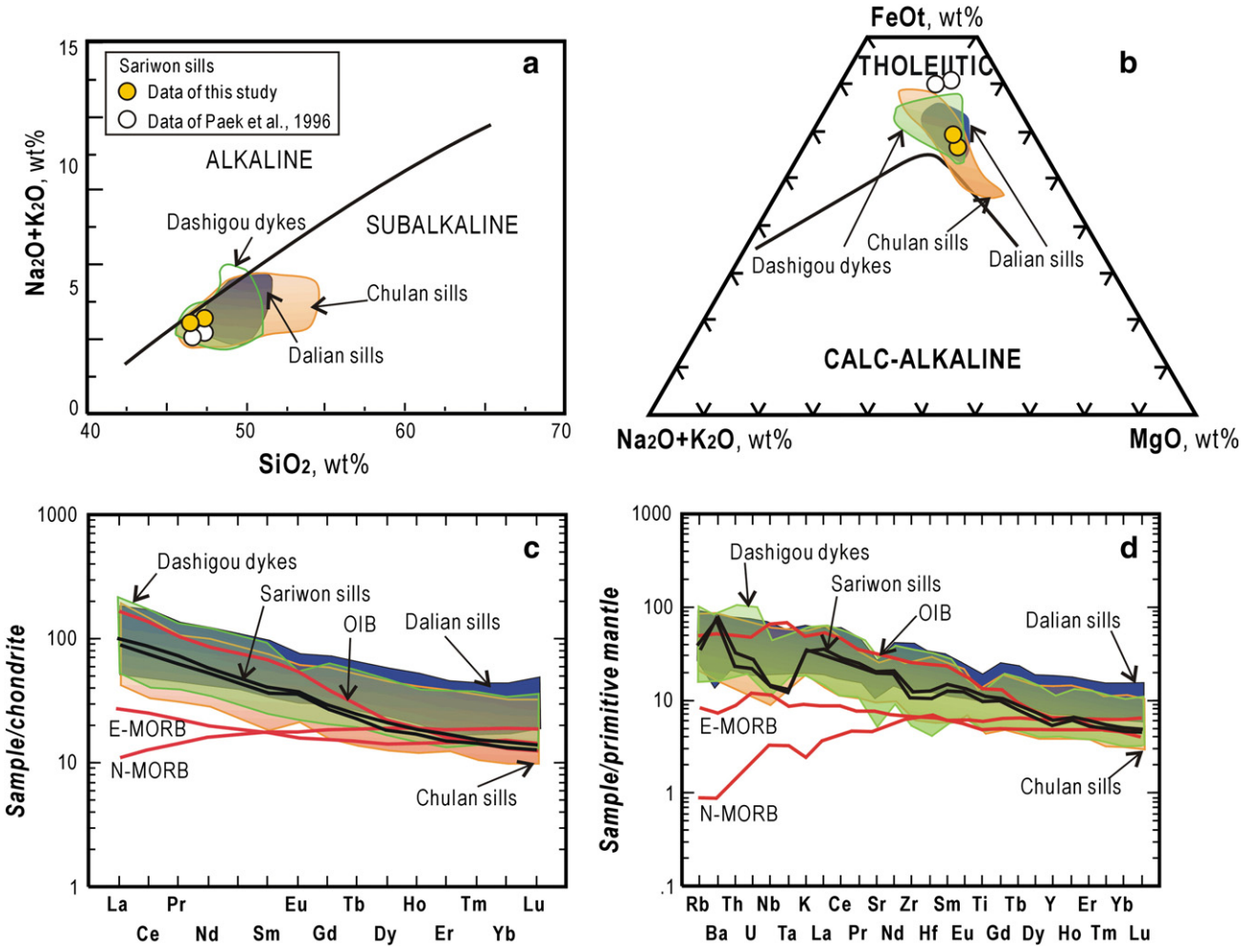

Fig. 5. (a) $Na_2O + K_2O$ versus SiO_2 diagram (after Irvine and Baragar, 1971); (b) FeOt–$Na_2O + K_2O$–MgO diagram (after Irvine and Baragar, 1971); (c) Chondrite-normalized rare earth element patterns; and (d) primitive mantle-normalized trace element spidergram of the Sariwon sills, as well as the Chulan sills (data of Pan et al., 2000a), Dalian sills (data of Yang et al., 2007), and Dashigou swarm (our unpublished data). Chondrite and primitive mantle-normalized values are after Sun and McDonough (1989).

sinistral displacement, the three swarms can be correlated (Fig. 7a) and therefore we consider the three swarms as part of a large sill swarm.

6.2. Comparison of the Xu–Huai, Lv–Da, and Pyongnam basins

Fig. 7a is a simplified geological map with the sinistral displacement of the two blocks on the opposite sides of the Tan-Lu fault reversed based on data supplied by Xu et al. (1987) and Xu (1993). After reconstruction, the Xu–Huai, Lv–Da and Pyongnam basins located side by side and are geographically connected. The ~918 Ma Chulan swarm intruded into the upper Xu–Huai and Bagongshan Groups in the Xu–Huai basin (Xuzhou–Huaibei basin) but is not seen in the Langan Group in this basin (BGMRA, 1985; Fig. 7a and b). According to BGMRA (1985), the Bagongshan Group is composed (from bottom to top) of conglomerate, quartz sandstone, mud-limestone, shales with limestone interlayers. The total thickness is about 600 m. The Xu–Huai Group consists (from bottom to top) of sandstone, limestone, and dolomite, and is about ~1500 m thick. The Shuxian Group is mainly composed of shale, sandstone, limestone and dolomite, and is about 880 m thick. The Langan Group contains a conglomerate layer in the bottom, but is otherwise composed of shales and dolomite and limestone, totaling about 140 m thick. We think the formations in the Xu–Huai Basin are comparable with those in the Pyongnam basin: the Bagongshan Group with the Jikhyon

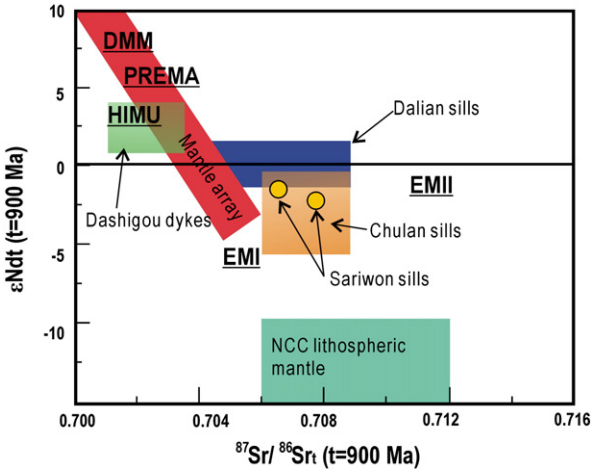

Fig. 6. Nd–Sr isotope diagram of the Sariwon sills, fields for the Chulan sills and Dashigou dyke swarm are after Pan et al. (2000a) and Peng et al. unpublished data. Field of the lithospheric mantle of the North China Craton is represented by the Taihang–Lvliang swarm for its large extension in the craton (data of Peng et al., 2007). DMM: depleted mantle, PREMA: prevalent mantle, HIMU: High U/Pb ratio mantle, EMI and EMII: Enriched Mantles I and II.

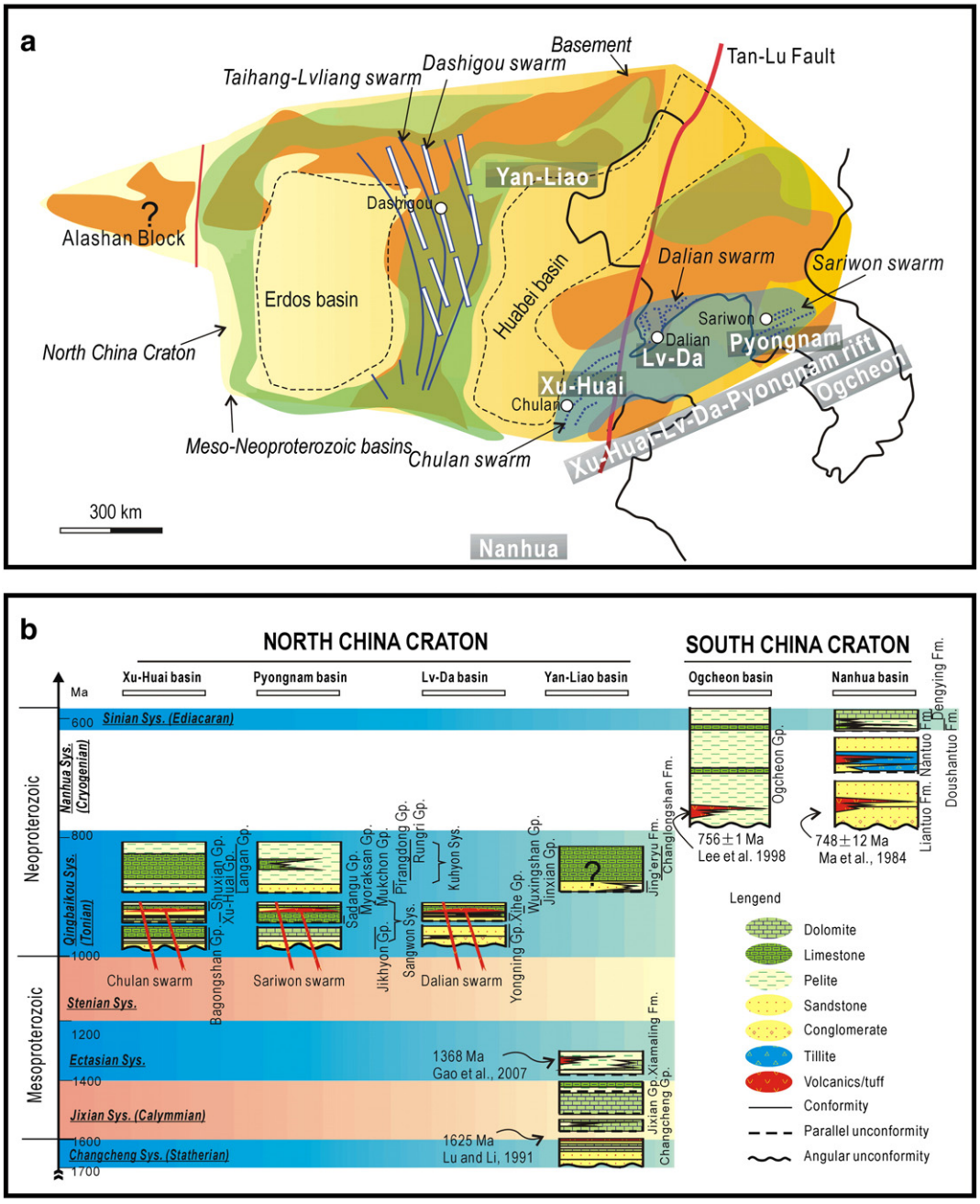

Fig. 7. (a) The North China Craton after reconstruction of the sinistral slip of the Tan-Lu fault (slip amount after Xu, 1993). The ~1780 Ma Taihang–Lvliang swarm, and ~900 Ma Dashigou, Chulan, Dalian and Sariwon swarms are also shown with sketched orientations. (b) Strata of representative basin formations in the North China craton and South China craton. Stratigraphy of Xu–Huai basin, Pyongnam basin, Lv–Da basin, Yan-Liao basin, Ogcheon basin, and Nanhua basin are revised based on this study and information from BGMRA (1985), Paek et al. (1996), BGMRL (1989), Gao et al. (2008), Fitches and Zhu (2006), and Wang and Li (2003), respectively.

Group, the Xu–Huai Group with the Sadangu Group, the Shuxian Group with the Myoraksan and Mukchon Groups, and the Langan Group with the Pirangdong and Rungri Groups (Kuhyon System) (Fig. 7b).

The sediments in the Lv–Da basin are composed of 4 groups, i.e., the Yongning Group, the Xihe Group, the Wuxingshan Group and the Jinxian Group (from bottom to top) (BGMRL, 1989). The ~900 Ma Dalian sills intruded the Wuxingshan and Jinxian Groups (BGMRL, 1989). The Yongning Group comprises conglomerate and sandstone, and varies in thickness from 500 to 6000 m. The Xihe Group contains sandstone, shales and quartzite, as well as some limestone interlayers, uncomformably overlain on the Yongning Group with a thin conglomerate layer. The thickness is about 800–1400 m. The Wuxingshan Group composes of sandstone, shale, dolostone and limestone, with a thickness of 750–1700 m. The Jinxian Group contains limestone with some shale layers. The thickness is about 600–1500 m. We think the Yongning Group is comparable with the Jikhyon Group, and the Xihe, Wuxingshan and Jinxian Groups are affinitive to the Sadangu, Myoraksan and Mukchon Groups in the Pyongnam basin, respectively (Fig. 7b).

As the Xu–Huai, Lv–Da and Pyongnam basins are geographically connected after reconstruction, and they contain comparable sediments, and in addition, all of them have sills with similar ages, we consider that the above three basins could belong to a single rift system, i.e. they composed a Xu–Huai–Lv–Da–Pyongnam (XLP) proto-basin during Neoproterozoic (Fig. 7a). It is worth mentioning that these basins are distinct from the Yan-Liao Basin in the NCC and Neoproterozoic basins in South China and southern Korean peninsula, which belong to the South China Craton, both in ages and in formations (e.g., Wang and

Li, 2003; Fitches and Zhu, 2006), e.g., they contain ~750 Ma volcanic layers (Nanhua basin in South China: Ma et al., 1984; Ogcheon basin in southern Korean peninsula: Lee et al., 1998) (Fig. 7b).

6.3. Implications for the evolution of the south-eastern margin of the NCC

The Chulan–Dalian–Sariwon sills have trace element patterns similar to ocean island basalts (OIB) (Fig. 5c and d), rather than those derived from the ancient sub-continental lithospheric mantle of the NCC (cf. Taihang–Lvliang dykes, Peng, 2010). In addition, Sr–Nd isotope data suggest that they have a magma source distinctly different from those from the lithospheric mantle of the NCC (Fig. 6). Fig. 4b shows *in-situ* zircon Hf isotopes from sample 05NK61, which give varied initial Hf isotopic ratios (Table 2). It is possible that some of these grains crystallized from a εHf_t depleted magma, the parental magma of the sills, and the varied εHf_t values represent isotopic ratios inherited/memorized from assimilated materials and/or of metamorphic disturbing. As the Sariwon sills, as well as the Chulan and Dalian sills show slightly depleted HFSEs (Fig. 5d) similar to those from continental crust (e.g. Gao et al., 1998), there would be varied amounts of contribution of crustal materials into their magma chambers. We suggest that the magma of the Chulan–Dalian–Sariwon sills was derived from asthenosphere, or a juvenile lithospheric mantle, but experienced crustal contamination. This agrees with their initial Nd isotopic natures (Fig. 6), i.e., they give values between DM (depleted mantle) sources and an ancient NCC lithospheric source. However, as Triassic syenite from the study area also show enriched Nd isotopic characteristics similar to those from the ancient NCC lithospheric mantle (Peng et al., 2008); this possibly indicates that the lithospheric mantle beneath the NCC was not rejuvenated till Triassic. Thus asthenosphere could be more likely the source of these sills, rather than a juvenile lithospheric mantle. The ~920 Ma Dashigou dyke swarm, which is located in the central part of the NCC, has a depleted magma source similar to the Chulan–Dalian–Sariwon sills (Fig. 6). This may indicate that there is a significant asthenosphere mantle upwelling under the NCC during Early Neoproterozoic, a proposal which warrants further study.

The possible geographic and genetic connection between the Pyongnam, Lv–Da and Xu–Huai basins suggest that there might be a single Neoproterozoic basin (the XLP proto-basin) that has been split by late tectonics (mainly due to strike–slip along the Tan-Lu fault). And the sills in this XLP proto-basin could be magma emplaced as a result of rifting during the deposition. Significant rifting along the south–eastern margin of the NCC during Neoproterozoic (~900 Ma) is suggested, although its extent in other parts of the NCC remains unclear.

The Chulan–Dalian–Sariwon sills and the Neoproterozoic strata in the Xu–Huai–Lv–Da–Pyongnam proto-basin have experienced deformation and greenschist-facies metamorphism (e.g., Paek et al., 1996). The lower intercept U–Pb zircon age of about 400 Ma (late Silurian to early Devonian) obtained from the Sariwon sill could provide for the age of this greenshist–facies metamorphism, which matches with some of the recently reported ~400 Ma granulite–facies metamorphic ages in the basement of the central part of the Korean peninsula (e.g., Cho, 2001; Sagong et al., 2003; Kim et al., 2006; Oh et al., 2009). Given the presence of the Qinling–Qilian orogen, along the southern part of the NCC, where a ~400 Ma collision event has been suggested (Fig. 1a; e.g. Sun et al., 2002; Yang et al., 2005), we suggest the effects of this collision also extended into the area of the southeastern NCC.

6.4. Implication for the configuration of the NCC in the Neoproterozoic supercontinent Rodinia

Neoproterozoic ages are rarely reported in the NCC, and thus it is in debating that whether or not the NCC has involved in the evolution of a Neoproterozoic supercontinent Rodinia (e.g., Zhai et al., 2003; Zhang et al., 2006). Yang et al. (2009) reported ~1.0 Ga ages from detrital zircons from sediments in the North China drainage area rivers, and have suggested a possible crustal growth episode in the NCC at that time. Ages from sills in this study confirm a significant magmatism event along the southeastern margin of the NCC. And these ~900 Ma marginal events could be possibly comparable and thus potentially connectable with those in some Rodinia pieces, e.g., the South China craton (e.g., Zhou et al., 2006; Ye et al., 2007; Li et al., 2009b), São Francisco craton (e.g., Uhlein et al., 1998), Nubian shield (e.g., Reischmann, 2000), Sri Lanka (e.g., Kröner et al., 2003), and so on. However, as the southeastern margin of the NCC was not metamorphosed and deformed from ~900 Ma till ~400 Ma, neither there is igneous event during this period; this margin was not likely a side facing the interior of the Rodinia in the configuration of this supercontinent.

7. Conclusions

We provide precise geochronological data on one of the Sariwon sills in the Pyongnam basin in the central Korean peninsula with a SIMS baddeleyite ^{206}Pb–^{207}Pb age of 899 ± 7 Ma. This sill swarm is coeval and show characteristics similar with the Chulan sills in the Xu–Huai basin and Dalian sills in the Lv–Da basin, and could be originally part of the same swarm. Bulk chemical features shows these sills might have originated from a depleted mantle source (e.g., asthenosphere, or a juvenile lithospheric mantle), suggesting significant mantle upwelling during Neoproterozoic under the NCC. Based on comparison of sedimentary formations in the Pyongnam, Xu–Huai and Lv–Da basins, we suggest that these rocks probably belonged to the same Neoproterozoic rift system (the Xu–Huai–Lv–Da–Pyongnam proto-basin). The sills, as well as the strata in the basins, have undergone late metamorphism and deformation, possibly at ~400 Ma and probably resulting from a continent-margin process along the southeastern margin of the NCC and can be linked with the Qinling–Qilian orogen located along the southern margin of the NCC. And the southeastern margin of the NCC was not likely a side facing the inland of the Rodinia in the configuration of this supercontinent.

Acknowledgements

This work benefits from cooperation with the Institute of Geology, The State Academy of Sciences, DPR Korea. Thanks are given to Drs. R Ernst and M Santosh for their help in improving an early version of this paper. This work is financially supported by grant nos. 90714003, 1731017007 and 41072146. Drs. XH. Li, GT. Hou and R. Srivastava are thanked for a constructive critique.

Appendix A

Representative mineral compositions of a Sariwon sill in North Korea.

	Minerals in the matrix		Minerals as inclusions in zircon grains			
	Clinopyroxene	Epidotite	Epidotite	Chlorite	albite	Feldspar
SiO_2	51.2225	38.8457	38.6637	23.5356	68.5163	63.2808
TiO_2	0.9462	0.1075	0.0041	0.0172	0.0244	0.0000
Al_2O_3	2.4175	25.8895	26.0842	19.4002	20.5806	20.0263
Cr_2O_3	0.1273	–	0.0051	0.0093	–	–
FeO	7.9786	8.5772	8.4443	34.3739	0.1208	2.3142
MgO	15.5641	0.0387	0.0356	9.8878	0.0110	0.2233
CaO	21.2547	21.8805	23.4683	0.0904	0.1882	2.9620
MnO	0.1858	0.1552	0.1149	0.1996	0.0213	0.0000
NiO	0.0478	–	0.0000	0.0261	–	–
Na_2O	0.2988	0.3500	0.0000	0.0000	7.6948	5.4743
K_2O	0.0116	0.0362	0.0237	0.0000	0.1056	0.1232

Appendix A (*continued*)

	Minerals in the matrix		Minerals as inclusions in zircon grains			
	Clinopyroxene	Epidotite	Epidotite	Chlorite	albite	Feldspar
H_2O	–	–	1.8636	10.7233	–	–
Cl	–	–	0.0205	–	–	–
total	100.0550	95.8805	98.7281	98.2634	97.2629	94.4041
Si	1.8952	2.0077	6.2031	5.2646	3.0231	2.9298
Ti	0.0263	0.0042	0.0005	0.0029	0.0008	0.0000
Al	0.1054	1.5770	4.9322	5.1144	1.0702	1.0928
Cr	0.0037	–	0.0007	0.0016	–	–
Fe	0.0697	–	–	–	–	–
Mg	0.8583	0.0030	0.0085	3.2966	0.0007	0.0154
Ca	0.8426	1.2116	4.0341	0.0217	0.0089	0.1469
Mn	0.0058	0.0068	0.0156	0.0378	0.0008	0.0000
Fe	0.1694	0.3707	1.1330	6.4302	0.0045	0.0896
Ni	0.0014	–	0.0000	0.0047	–	–
Na	0.0214	0.0351	0.0000	0.0000	0.6583	0.4914
K	0.0005	0.0024	0.0048	0.0000	0.0059	0.0073
total	4.0000	5.2184	16.3324	20.1745	4.7731	4.7732

Note: 1. blanks with "–" refer to those under determination limitation or not measured. 2. Analysis finished in the Institute of Geology and Geophysics, Chinese Academy of Sciences, using a CAMECA SX51 machine.

References

Black, L.P., Kamo, S.L., Allen, C.M., Aleinikoff, J.N., Davis, D.W., Korsch, R.J., Foudoulis, C., 2003. TEMORA 1: a new zircon standard for Phanerozoic U–Pb geochronology. Chemical Geology 200, 155–170.

Blichert-Toft, J., Albarède, F., 1997. The Lu–Hf geochemistry of chondrites and the evolution of the mantle–crust system. Earth and Planetary Science Letters 148, 243–258.

Bureau of Geology and Mineral Resources of Anhui (BGMRA), 1985. Strata of Anhui (Precambrian part). Anhui Science and Technology Publishing House, Hefei. 174pp.

Bureau of Geology and Mineral Resources of Liaoning (BGMRL), 1989. Regional Geology of Liaoning Province. Geological Publishing House, Beijing. 856pp.

Chang, K.H., Park, S.O., 2001. Paleozoic Yellow Sea Transform Fault: its role in the tectonic history of Korea and adjacent regions. Gondwana Research 4, 588–589.

Cheong, C.-S., Jeong, G.Y., Kim, H., Choi, M.S., Lee, S.H., Cho, M., 2003. Early Permian peak metamorphism recorded in the U–Pb system of black slates from the Ogcheon metamorphic belt, South Korea, and its tectonic implications. Chemical Geology 193, 81–92.

Chesworth, W., Dejou, J., Larroque, P., 1981. The weathering of basalt and relative motilities of the major elements at Belbex, France. Geochimica et Cosmochimica Acta 45 (7), 1235–1243.

Cho, M., 2001. A continuation of Chinese ultrahigh-pressure belt in Korea: evidence from ion microprobe U–Pb zircon ages. Gondwana Research 4, 708.

Cho, M., Kwon, S.T., Ree, J.H., Nakamura, E., 1995. High-pressure amphibolite of the Imjinggang belt in the Yeoncheon–Cheongok area. Journal of Petrological Society of Korea 4, 1–19.

Choi, S.-C., Oh, C.-W., Luehr, H., 2006. Tectonic relation between northeastern China and the Korean peninsula revealed by interpretation of GRACE satellite gravity data. Gondwana Research 9, 62–67.

Chough, S.-K., Kwon, S.-T., Ree, J.-H., Choi, D.K., 2000. Tectonic and sedimentary evolution of the Korean peninsula: a review and new view. Earth Science Reviews 52, 175–235.

Chun, S.S., Chough, S.K., 1992. Tectonic history of Cretaceous sedimentary basins in the southwestern Korean Peninsula and Yellow Sea. In: Chough, S.K. (Ed.), Sedimentary Basins in the Korean Peninsula and Adjacent Seas. : Korean Sediment. Research Group Special Publication. Harnlimwon Publishers, Seoul, pp. 60–76.

DePaolo, D.J., 1981. Nd isotopes in the Colorado Front Range and crust–mantle evolution in the Proterozoic. Nature 291, 193–196.

Fitches, W.R., Zhu, G., 2006. Is the Ogcheon metamorphic belt of Korea the eastward continuation of the Nanhua Basin of China? Gondwana Research 9, 68–84.

Gao, L.-Z., Zhang, C.-H., Shi, X.-Y., Zhou, H.-R., Wang, Z.-Q., 2007. Zircon SHRIMP U–Pb dating of the tuff bed in the Xiamaling Formation of the Qingbaikou System in North China. Geological Bulletin of China 26 (3), 249–255 (in Chinese with English abstract).

Gao, L.-Z., Zhang, C.-H., Yin, C.-Y., Shi, X.-Y., Wang, Z.-Q., Liu, Y.-M., Liu, P.-J., Tang, F., Song, B., 2008. SHRIMP zircon ages: basis for refining the chronostratigraphic classification of the Meso- and Neoproterozoic Strata in North China Old Land. Acta Geoscientica Sinica 29 (3), 366–376 (In Chinese with English abstract).

Gao, S., Luo, T.-H., Zhang, B.-R., Zhang, H.-F., Han, Y.-W., Zhao, Z.-D., Hu, Y.-K., 1998. Chemical compositions of the continental crust as revealed by sudies in East China. Geochmica et Cosmochimica Acta 62, 1959–1975.

Griffin, W.L., Pearson, N.J., Belousova, E., Jackson, S.E., van Achterbergh, E., O'Reilly, S.Y., Shee, S.R., 2000. The Hf isotope composition of cratonic mantle: LAM-MC-ICPMS analysis of zircon megacrysts in kimberlites. Geochimica et Cosmochimica Acta 64 (1), 133–147.

Heaman, L.M., LeCheminant, A.N., 1993. Paragenesis and U–Pb systematics of baddeleyite (ZrO_2). Chemical Geology 110, 95–126.

Hou, G.-T., Liu, Y.-L., Li, J.-H., Jin, A.-W., 2005. The SHRIMP U-Pb chronology of mafic dyke swarms: a case study of Laiwu diabase dykes in western Shandong. Acta Petrologica et Mineralogica 24 (3), 179–185 (in Chinese with English abstract).

Hou, Q.-L., Wu, F.-Y., Zhai, M.-G., Guo, J.-H., Li, Z., 2008. Possible tectonic manifestations of the Dabie–Sulu orogenic blet on the Korean Peninsula. Geological Bulletin of China 27 (10), 1659–1666.

Ishiwatari, A., Tsujimori, T., 2003. Paleozoic ophiolites and blueschists in Japan and Russian Primorye in the tectonic framework of East Asia: a synthesis. Island Arc 12, 190–206.

Irvine, T.N., Baragar, W.R.A., 1971. A guide to the chemical classification of the common volcanic rocks. Canadian Journal of Earth Sciences 8, 523–548.

Kim, S.-W., Oh, C.-W., Williams, I.S., Rubatto, D., Ryu, I.-C., Rajesh, V.J., Kim, C.-B., Guo, J.-H., Zhai, M.-G., 2006. Phanerozoic high-pressure eclogite and intermediate-pressure granulite facies metamorphism in the Gyeonggi Massif, South Korea: implications for the eastward extension of the Dabie–Sulu continental collision zone. Lithos 92, 357–377.

Kim, S.W., Kown, S., Ryu, I.-C., 2009. Geochronological constraints on multiple deformations of the Honam Shear Zone, South Korea and its tectonic implication. Gondwana Research 16, 82–89.

Kröner, Kehelpannala, K.V.W., Hegner, E., 2003. Ca. 750–1100 Ma magmatic events and Grenville-age deformation in Sri Lanka: relevance for Rodinia supercontinent formation and dispersal, and Gondwana amalgamation. Journal of Asian Earth Sciences 22, 279–300.

Kwon, S., Sakeev, K., Mitra, G., Park, Y., Kim, S.W., Ryu, I.-C., 2009. Evidence for Permo-Triassic collision in Far East Asia: the Korean collisional orogen. Earth and Planetary Science Letters 279 (3–4), 340–349.

Lee, K.S., Chang, H.W., Park, K.H., 1998. Neoproterozoic bimodal volcanism in the central Ogcheon belt, Korea: age and tectonic implication. Precambrian Research 89, 47–57.

Li, Q.L., Li, X.H., Liu, Y., Tang, G.Q., Yang, J.H., Zhu, W.G., 2010. Precise U–Pb and Pb–Pb dating of Phanerozoic baddeleyite by SIMS with oxygen flooding technique. Journal of Analytical Atomic Spectrometry 25, 1107–1113.

Li, X.-H., Liu, Y., Li, Q.-L., Guo, C.-H., Chamberlain, K.R., 2009a. Precise determination of Phanerozoic zircon Pb/Pb age by multicollector SIMS without external standardization. Geochemistry Geophysics Geosystem 10, Q04010, doi:10.1029/2009GC002400.

Li, X.-H., Li, W.-X., Li, Z.-X., Lo, Q.-H., Wang, J., Ye, M.-F., Yang, Y.-H., 2009b. Amalgamation between the Yangtze and Cathaysia Blocks in South China: constraints from SHRIMP U–Pb zircon ages, geochemistry and Nd–Hf isotopes of the Shuangxiwu volcanic rocks. Precambrian Research 174, 117–128.

Liu, D.-Y., Nutman, A.P., Compston, W., Wu, J.-S., Shen, Q.-H., 1992. Remnants of 3800 Ma crust in the Chinese part of the Sino-Korean Craton. Geology 20, 339–342.

Liu, D.-Y., Wilde, S., Wan, Y.-S., Wu, J.-S., Zhou, H.-Y., Dong, C.-Y., Yin, X.-Y., 2008. New U–Pb and Hf isotopic data confirm Anshan as the oldest preserved segment of the North China craton. American Journal of Science 308, 200–231.

Liu, Y.-Q., Gao, L.-Z., Liu, Y.-X., Song, B., Wang, Z.-X., 2006. Zircon U–Pb dating for the earliest Neoproterozoic mafic magmatism in the southern margin of the North China Block. Chinese Science Bulletin 51 (19), 2375–2382.

Lu, S.N., Li, H.M., 1991. A precise U–Pb single zircon age determination for the volcanics of the Dahongyu Formation, Changcheng System in Jinxian. Bulletin. Chinese Academy of Geological Science 22, 137–145 (Chinese with English abstract).

Lu, S.-N., Zhao, G.-C., Wang, H.-C., Hao, G.-J., 2008. Precambrian metamorphic basement and sedimentary cover of the North China Craton: a review. Precambrian Research 160, 77–93.

Ludwig, K.R., 2002. SQUID 1.02, A User's Manual. Berkeley Geochronology Center, Special Publication No 2. .

Ludwig, K.R., 2003. User's Manual for Isoplot/EX Version 3.00. A Geochronological Toolkit for Microsoft Excel, vol. 4. Berkeley Geochronology Center Special Publication. 71 pp.

Ma, G., Li, H., Zhang, Z., 1984. An investigation of the age limits of the Sinian System in South China. Bulletin of Yichang Institute of Geology Mineral Resources 8, 1–29 (in Chinese with English abstract).

Middelburg, J.J., Van derWeijden, C.H., Woittiez, J.R.W., 1988. Chemical processes affecting the mobility of major, minor and trace elements during weathering of granitic rocks. Chemical Geology 68, 253–273.

Oh, C.W., 2006. A new concept on tectonic correlation between Korea, China, and Japan: histories from the Late Proterozoic to Cretaceous. Gondwana Research 9, 47–61.

Oh, C.-W., Choi, S.-G., Seo, J., Rajesh, V.J., Lee, J.-H., Zhai, M., Peng, P., 2009. Neoproterozoic tectonic evolution of the Hongseong area, southwestern Gyeonggi Massif, South Korea; implication for the tectonic evolution of Northeast Asia. Gondwana Research 16 (2), 272–284.

Oh, C.W., Kim, S.W., Choi, S.-G., Zhai, M., Guo, J., Sajeev, K., 2005. First finding of eclogite facies metamorphic event in South Korea and its correlation with the Dabie–Sulu collision belt in China. Journal of Geology 113, 226–232.

Oh, C.W., Kusky, T., 2007. The late Permian to Triassic Hongseong–Odesan Collision Belt in South Korea, and its tectonic correlation with China and Japan. International Geology Review 49, 636–657.

Paek, R.-J., Gap, K.-H., Jon, G.-P. (Eds.), 1996. Geology of Korea. Foreign Languages Books Publishing House, Pyongyang. 631pp.

Pan, G.-Q., Kong, Q.-Y., Wu, Q.-Q., Liu, J.-R., Zhang, Q.-L., Zeng, J.-H., Liu, D.-Z., 2000a. Geochemical Features of Neoproterozoic Diabase Sills in Xuzhou–Suzhou area. Geological Journal of China Universities 6 (1), 53–63 (in Chinese with English abstract).

Pan, G.-Q., Liu, J.-R., Kong, Q.-Y., Wu, Q.-Q., Zhang, Q.-L., Zeng, J.-H., Liu, D.-Z., 2000b. Study on Sinian geologic events in Xuzhou–Suzhou Area and discussion on their

origin. Geological Journal of China Universities 6 (4), 566–575 (in Chinese with English abstract).
Pandarinath, K., Dulski, P., Torres-Alvarado, I.S., Verma, S.P., 2008. Element mobility during the hydrothermal alteration of rhyolitic rocks of the Los Azufres geothermal field, Mexico. Geothermics 37, 53–72.
Peng, P., Zhai, M.-G., Guo, J.-H., Zhang, H.-F., Zhang, Y.-B., 2008. Petrogenesis of Triassic postorogenic syenite plutons in the Sino-Korean craton: an example from North Korea. Geological Magazine 145 (5), 637–647.
Peng, P., Zhai, M.-G., Guo, J.-H., Kusky, T., Zhao, T.-P., 2007. Nature of mantle source contributions and crystal differentiation in the petrogenesis of the 1.78 Ga mafic dykes in the central North China craton. Gondwana Research 12, 29–46.
Peng, P., 2010. Reconstruction and interpretation of giant mafic dyke swarms: a case study of 1.78 Ga magmatism in the North China craton. In: Kusky, T., Zhai, M.-G., Xiao, W.-J. (Eds.), The Evolving Continents: Understanding Processes of Continental Growth: Geological Society, London, Special Publications, 338, pp. 163–178.
Qiao, X.-F., Gao, L.-Z., Zhang, C.-H., 2007. New idea of the Meso- and Neoproterozoic chronostratigraphic chart and tectonic environment in Sino-Korean Plate. Geological Bulletin of China 26 (5), 503–509 (in Chinese with English abstract).
Reischmann, T., 2000. Ophiolites and island arcs in the late Proterozoic Nubian Shield. Ofioli 25, 1–13.
Ree, J.H., Cho, M., Kwon, S.T., Nakamura, E., 1996. Possible eastward extension of Chinese collision belt in South Korea: the Imjinggang belt. Geology 24, 1071–1074.
Ryu, J.-P., Kang, M.-S., Kim, J.-P., Tongbang, G.U., Jang, T.-G., Song, Y.-P., Kwon, J.-R., 1990. Geological Constitution of Korea, 4. Industrial Publishing House, Pyeongyang. 304pp.
Sagong, H., Cheong, C.-S., Kwon, S.-T., 2003. Paleoproterozoic orogeny in South Korea: evidence from Sm–Nd and Pb step-leaching garnet ages of Precambrian basement rocks. Precambrian Research 122, 1–21.
Sajeev, K., Jeong, J., Kwon, S., Kee, W.-S., Kim, S.W., Komiya, T., Itaya, T., Jug, H.-S., Park, Y., 2010. High P–T granulite relicts from the Imjingang belt, South Korea: tectonic significance. Gondwana Research 17, 75–86.
Söderlund, U., Patchett, P.J., Vervoort, J.D., Isachsen, C.E., 2004. The ^{176}Lu decay constant determined by Lu–Hf and U–Pb isotope systematics of Precambrian mafic intrusions. Earth and Planetary Science Letters 219, 311–324.
Sun, S.-S., McDonough, W.F., 1989. Chemical and isotopic systematics of oceanic basalts implications for mantle composition and process. In: Saunders, A.D., Nony, M.J. (Eds.), Magmatism in the Ocean Basins: Geological Society Special Publication, 42, pp. 313–354.
Sun, W., Williams, I.S., Li, S., 2002. Carboniferous and Triassic eclogites in the western Dabie Mountains, east-central China: evidence for protracted convergence of the North and South China Blocks. Journal of Metamorphism Geology 20, 873–886.
Uhlein, A., Trompette, R.R., Egydio-Silva, M., 1998. Proterozoic rifting and closure, SE border of the São Francisco Craton, Brazil. Journal of South American Earth Sciences 11, 191–203.
Wang, J., Li, Z.-X., 2003. History of Neoproterozoic rift basins in South China: implications for Rodinia break-up. Precambrian Research 122, 141–158.
Williams, I.S., 1998. U–Th–Pb geochronology by ion microprobe, Applications of microanalytical techniques to understanding mineralizing processes. In: McKibben, M.A., Shanks, W.C., Ridley, W.I. (Eds.), Review of Economic Geology, 7, pp. 1–35.
Wingate, M.T.D., Compston, W., 2000. Crystal orientation effects during ion microprobe U–Pb analysis of baddeleyite. Chemical Geology 168, 75–97.
Wu, F.-Y., Zhang, Y.-B., Yang, J.-H., Xie, L.-W., Yang, Y.-H., 2008. Zircon U–Pb and Hf isotopic constraints on the Early Archean crustal evolution in Anshan of the North China Craton. Precambrian Research 167 (3–4), 339–362.
Wu, F.-Y., Han, R.-Y., Yang, J.-H., Wilde, S.A., Zhai, M.-G., Park, S.-C., 2007. Initial constraints on the timing of granitic magmatism in North Korea using U–Pb zircon geochronology. Chemical Geology 238, 232–248.
Wu, F.Y., Yang, Y.H., Xie, L.W., Yang, J.H., Xu, P., 2006. Hf isotopic compositions of the standard zircons and baddeleyites used in U–Pb geochronology. Chemical Geology 234, 105–126.
Xu, J.W., Zhu, G., Tong, W., Cui, K., Liu, Q., 1987. Formation and evolution of the Tancheng–Lujiang wrench fault system: a major shear system to the northeast of the Pacific Ocean. Tectonophysics 134, 273–310.
Xu, J.-W., Zhu, G., 1995. Discussion on tectonic models for the Tan-Lu fault zone, Eastern China. Journal of Geology and Mineral Resources of North China 10, 121–133 (in Chinese).
Xu, J.W., 1993. The Tancheng–LujiangWrench Fault System. Wiley, New York. 279 p.
Yang, J., Gao, S., Chen, C., Tang, Y.-Y., Yuan, H.-L., Gong, H.-J., Xie, S.-W., Wang, J.-Q., 2009. Episodic crustal growth of North China as revealed by U–Pb age and Hf isotopes of detrital zircons from modern rivers. Geochimica et Cosmochimica Acta 73, 2660–2673.
Yang, J., Liu, F., Wu, C., Xu, Z., Shi, R., Chen, S., 2005. Two ultrahigh-pressure metamorphic events recognized in the central orogenic belt of China: evidence from the U–Pb dating of coesite-bearing zircons. International Geological Review 47, 327–343.
Yang, J.-H., Sun, J.-F., Chen, F.-K., Wilde, S., Wu, F.-Y., 2007. Sources and petrogenesis of Late Triassic dolerite dikes in the Liaodong peninsula: implications for post-collisional lithosphere thinning of the Eastern North China craton. Journal of Petrology 48 (10), 1973–1997.
Yang, J.-H., Wu, F.-Y., Zhang, Y.-B., Zhang, Q., Wilde, S.A., 2004. Identification of Mesoproterozoic zircons in a Triassic dolerite from the Liaodong Peninsula, East China. Chinese Science Bulletin 49, 1878–1882.
Ye, M.-F., Li, X.-H., Li, W.-X., Liu, Y., Li, Z.-X., 2007. SHRIMP zircon U–Pb geochronological and whole-rock geochemical evidence for an early Neoproterozoic Sibaoan magmatic arc along the southeastern margin of the Yangtze Block. Gondwana Research 12, 144–156.
Yin, A., Nie, S., 1993. An indentation model for the north and south China collision and the development of the Tan-Lu and Honam fault systems, Eastern Asian. Tectonics 12, 801–813.
Zhai, M.-G., Guo, J.-H., Li, Z., Chen, D.-Z., Peng, P., Li, T.-S., Hou, Q.-L., Fan, Q.-C., 2007. Linking the Sulu UHP belt to the Korean Peninsula: evidence of eclogite, Precambrian basement, and Paleozoic sedimentary basins. Gondwana Research 12, 388–403.
Zhai, M.-G., Shao, J.-A., Hao, J., Peng, P., 2003. Geological signature and possible position of the North China block in the Supercontinent Rodinia. Gondwana Research 6, 171–183.
Zhang, S.-H., Li, Z.-X., Wu, H.-C., 2006. New Precambrian palaeomagnetic constraints on the position of the North China Block in Rodinia. Precambrian Research 144, 213–238.
Zhou, Meifu, Ma, Yuxiao, Yan, Danping, Xia, Xiaoping, Zhao, Junhong, Sun, Min, 2006. The Yanbian terrane (Southern Sichuan Province, SW China): a Neoproterozoic arc assemblage in the western margin of the Yangtze block. Precambrian Research 144, 19–38.